ISBN: 978-3-95450-184-7 doi:10.18429/JACoW-IPAC2018-THPAK036

ACCURATE MODELING OF FRINGE FIELD EFFECTS ON NONLINEAR INTEGRABLE OPTICS IN IOTA

C. E. Mitchell*, R. D. Ryne, Lawrence Berkeley National Laboratory, Berkeley, CA, USA
F. H. O'Shea, RadiaBeam, Santa Monica, CA, USA

Abstract

The Integrable Optics Test Accelerator (IOTA) is a novel storage ring under commissioning at Fermi National Accelerator Laboratory designed to investigate the dynamics of beams with large transverse tune spread in the presence of strongly nonlinear integrable optics [1, 2]. Nonlinear multipole errors resulting from magnetic fringe fields can impact the integrability of particle motion, and long-term numerical tracking requires an accurate representation of these effects. Surface fitting algorithms provide a robust and reliable method for extracting this information from 3-dimensional magnetic field data provided on a grid. These algorithms are applied to investigate the unique nonlinear magnetic insert of the IOTA ring, and consequences of the fringe fields to the long-term dynamics of the beam are discussed.

INTRODUCTION

Integrable particle motion with large transverse tune spread in IOTA will be achieved by introducing a 1.8 m long insert with strongly nonlinear $s-$dependent transverse magnetic field into a zero-dispersion section of the IOTA ring [2]. This magnetic insert has been designed to within tight tolerances [3], and must be properly matched to the underlying linear lattice to ensure integrability. Tracking studies for IOTA have primarily used simplified or idealized models of the nonlinear insert. In this paper, we describe a method for including the effects of realistic 3D magnetic fringe fields.

Cylindrical Harmonics and Generalized Gradients

A general 3D magnetostatic field in a source-free region may be expressed as $\vec{B} = \nabla\times\vec{A} = -\nabla\psi$, where the magnetic scalar potential ψ is given in cylindrical coordinates in the form:

$$\psi(\rho,\phi,s) = -\sum_{l=0}^{\infty}\sum_{m=0}^{\infty}(-1)^l\frac{m!}{2^{2l}l!(l+m)!}\rho^{2l+m} \times\left[C_{m,s}^{[2l]}(s)\sin(m\phi)+C_{m,c}^{[2l]}(s)\cos(m\phi)\right]. \quad (1)$$

Here s denotes the longitudinal coordinate, and the functions $C_{m,\alpha}^{[2l]}$ ($\alpha = s,c$), known as *on-axis generalized gradients*, characterize the magnetic field completely with:

$$C_{m,\alpha}^{[n]}(s) = \frac{d^n}{ds^n}C_{m,\alpha}^{[0]}(s). \quad (2)$$

The representation (1) provides a concise Maxwellian description of the field, while the functions $C_{m,\alpha}^{[2l]}$ may be used to construct corresponding series of the form (1) for the magnetic vector potential, as required for symplectic tracking or symplectic map analysis [4].

FIELD AND POTENTIALS OF THE IDEAL NONLINEAR MAGNETIC INSERT

We first analyze the generalized gradients for the "ideal" nonlinear insert, described at each longitudinal location s by a 2D magnetic field $\vec{B} = B_x\hat{x}+B_y\hat{y}$ satisfying $\partial_x B_x+\partial_y B_y = 0$ and $\partial_x B_y - \partial_y B_x = 0$. This field is most easily expressed in terms of either a magnetic vector potential $\vec{A} = A_s\hat{s}$ or a magnetic scalar potential ψ satisfying $\vec{B} = \nabla_\perp\times\vec{A} = -\nabla_\perp\psi$ at each s, where the two potentials are given by the real and imaginary parts of the function [5]:

$$F(z) = \left(\frac{\tilde{t}z}{\sqrt{1-z^2}}\right)\arcsin(z), \quad (3)$$

in terms of the dimensionless quantities:

$$F = \frac{A_s+i\psi}{B\rho}, \quad z = \frac{x+iy}{c\sqrt{\beta(s)}}, \quad \tilde{t} = \frac{\tau c^2}{\beta(s)}. \quad (4)$$

Here τ denotes a dimensionless nonlinear insert strength, c [$m^{1/2}$] characterizes the transverse scale of the nonlinear insert, and $\beta(s)$ denotes the horizontal=vertical betatron amplitude within the drift space that will contain the nonlinear insert, which is given explicitly by:

$$\frac{\beta(s)}{\beta^*} = 1+\left(\frac{2s}{L}\right)^2\tan^2\pi\mu_0, \quad \text{for} \quad -\frac{L}{2}\le s\le\frac{L}{2}. \quad (5)$$

In (5), L denotes the length of the nonlinear insert, $0\le\mu_0<0.5$ denotes the tune advance across the nonlinear insert, and β^* denotes the betatron amplitude at the midpoint of the nonlinear insert, given in terms of the parameters L and μ_0 by:

$$\beta^* = \frac{L}{2}\cot\pi\mu_0. \quad (6)$$

Due to the s-dependence of the betatron amplitude β appearing in (4-5), the "ideal" magnetic scalar potential does not satisfy the 3D Laplace equation: $\nabla^2\psi\neq\nabla_\perp^2\psi = 0$. To represent the fields in the form (1), we must assume that the longitudinal derivatives in (1) are negligible, so that $C_{m,\alpha}^{[2l]}(s) = 0$ for $\alpha = s,c$ and $l\ge 1$. Comparing (1) with the power series for (3) and equating terms of like degree, we find that the generalized gradients describing the ideal

* ChadMitchell@lbl.gov

ISBN: 978-3-95450-184-7 doi:10.18429/JACoW-IPAC2018-THPAK036

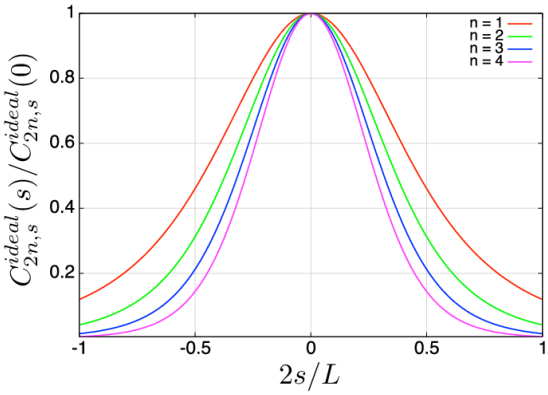

Figure 1: The first four of the nonvanishing generalized gradients (7) are shown for the ideal IOTA nonlinear insert for the case $\mu_0 = 0.3$. In each case, the quantity $C^{ideal}_{2n,s}$ is normalized by its value at the longitudinal midpoint.

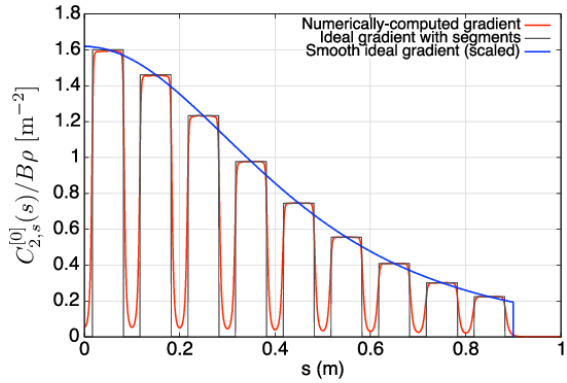

Figure 2: The lowest-order nonvanishing generalized gradient (7) is shown for the IOTA nonlinear insert prototype (red), together with its ideal counterpart (7) (blue) and its approximation by segments (black).

nonlinear magnetic insert are given (in physical units) for $n \geq 1$ by:

$$C^{ideal}_{2n,s}(s) = -\tau \left(\frac{B\rho}{c^{4n}}\right) \frac{2^{2n-1} n!(n-1)!}{(2n)!} \left(\frac{c^2}{\beta(s)}\right)^{n+1}, \quad (7)$$

with $C^{ideal}_{m,s} = 0$ for odd m and $C^{ideal}_{m,c} = 0$ for all m. Fig. 1 illustrates the first four of the quantities (7) evaluated for an insert tune advance of $\mu_0 = 0.3$. Note that these quantities drop discontinuously to zero at the endpoints $s = \pm L/2$. The quantities become more sharply peaked about the midpoint of the magnet with increasing n. At each fixed s, the domain of convergence of the series (1) is given by $|z| < 1$, where z was defined in (4).

ANALYSIS OF 3D MAGNETIC FIELD DATA USING SURFACE METHODS

Computation of Generalized Gradients

The physical magnetic insert consists of 18 segments of length 6.5 cm separated by 3.5 cm gaps. Table 1 contains the basic parameters to which the magnetic insert was designed [6]. Using ANSYS, numerically-computed magnetic field values were provided on the surface of a circular cylinder (within the vacuum chamber) of radius 4.8 mm surrounding the magnetic axis (32×1601 points over a single octant). To mitigate difficulties associated with numerical noise, a surface-fitting method [4] was used to extract generalized gradients through order $m = 8$. Explicitly,

$$C^{[n]}_{m,\alpha}(s) = \frac{i^n}{2^m m!} \int_{-\infty}^{\infty} \frac{k^{n+m-1}}{I'_m(kR)} \tilde{B}^{\alpha}_{\rho}(R,m,k) e^{iks} dk, \quad (8)$$

where

$$\tilde{B}^{s}_{\rho}(R,m,k) = \frac{1}{2\pi^2} \int_{-\infty}^{\infty} \int_{0}^{2\pi} e^{-iks} \sin(m\phi) B_{\rho}(R,\phi,s) d\phi ds,$$

with a corresponding expression for $\tilde{B}^{c}_{\rho}$. It was necessary to use a large cutoff in the frequency domain ($k_{\max}$=4.2 mm^{-1}, 7001 samples) to resolve peaks in the magnetic field on the surface of the cylinder near the pole faces associated with transitions between segments.

Table 1: Nominal Design Parameters of the IOTA Nonlinear Insert (NLI) Prototype

Parameter	Symbol	Value
Strength parameter	τ	0.45
Transverse scale factor	c	0.009 m$^{1/2}$
Tune advance across NLI	μ_0	0.3
Length of NLI	L	1.8 m
Beta at NLI midpoint	β^*	0.6538 m
Segment length	Δs	6.5 cm

Figure 2 illustrates the lowest-order nonvanishing gradient, together with its ideal counterpart from (7). The ideal gradient has been scaled by a factor of $f = 1.54$ (segment separation/segment length) to account for the fact that the strength of the field in each segment has been increased to produce the same integrated kick that would occur if the segments were not separated by gaps.

Applying the Fringe Field Correction

The exact Hamiltonian within the nonlinear insert, using longitudinal position s as the independent variable, is given by:

$$H = -\sqrt{1 - \frac{2P_t}{\beta_0} + P_t^2 - (\vec{P} - \vec{\mathcal{A}}_{\perp})^2} - \mathcal{A}_s - \frac{1}{\beta_0} P_t, \quad (9)$$

where the transverse momenta $\vec{P}$ are normalized by the design momentum $p^0 = mc\beta_0\gamma_0$, the longitudinal variables are $T = c\Delta t$ and $P_t = -\Delta\gamma/(\beta_0\gamma_0)$, and $\vec{\mathcal{A}} = \vec{A}/B\rho$. The ideal (integrable) Hamiltonian within the nonlinear insert is given by:

$$H^{ideal} = \frac{1}{2}(P_x^2 + P_y^2) - \mathcal{A}_s^{ideal}(X,Y,s). \quad (10)$$

ISBN: 978-3-95450-184-7 doi:10.18429/JACoW-IPAC2018-THPAK036

To include the effect of segments and gaps, we also consider

$$H^{seg} = \frac{1}{2}(P_x^2 + P_y^2) - \chi(s)\mathcal{A}_s^{ideal}(X, Y, s_m(s)), \quad (11)$$

where $\chi(s) = f$ within each segment, and $\chi(s) = 0$ elsewhere. Here $s_m(s)$ denotes the longitudinal location at the midpoint of that segment nearest to s. One may apply a fringe field correction of degree N to the Hamiltonian (11) by using instead the Hamiltonian

$$H^{frg} = H^{seg} + \Delta H_N, \quad (12)$$

where ΔH_N denotes the difference $H - H^{seg}$, expressed through terms of degree N. This requires evaluating Taylor series in X and Y for the vector potentials $\vec{\mathcal{A}}$ and $\vec{\mathcal{A}}^{ideal}$, whose coefficients are obtained directly from the on-axis generalized gradients $C_{m,\alpha}^{[n]}$ ($\alpha = s, c$) [4]. In this study, we investigate the effect of those correction terms containing $C_{2,s}^{[0]}$ (quadrupole errors) and $C_{4,s}^{[0]}$ (octupole errors) only. Sextupole errors vanish due to symmetry.

TRACKING RESULTS

We initialize a 2.5 MeV proton beam at the entrance to the nonlinear insert with a matched KV-type distribution of the form $f \propto \delta(H^{ideal} - \epsilon_0)$, where $\epsilon_0 = 4$ mm-mrad. To isolate the effect of the nonlinear insert fringe fields, the beam is tracked without space charge in a toy benchmark lattice, in which all elements external to the nonlinear magnetic insert are replaced by a single linear isotropic focusing kick [1]. Symplectic tracking [7] is used within the nonlinear insert with a large number of longitudinal steps (3840) to resolve fringe field variation between segments. Fig. 3 shows the evolution of the moments of the two invariants of motion [1], taken among all particles in the beam. After an initial redistribution of the invariants over the first 1,000 turns, the beam settles into a quasi-steady-state, after which there is little evidence of the slow secular growth associated with chaotic diffusion. A small number of particles experience net increases in amplitude as large as 10-20% (Fig. 4), which occur before turn 1,000 with little visible change thereafter.

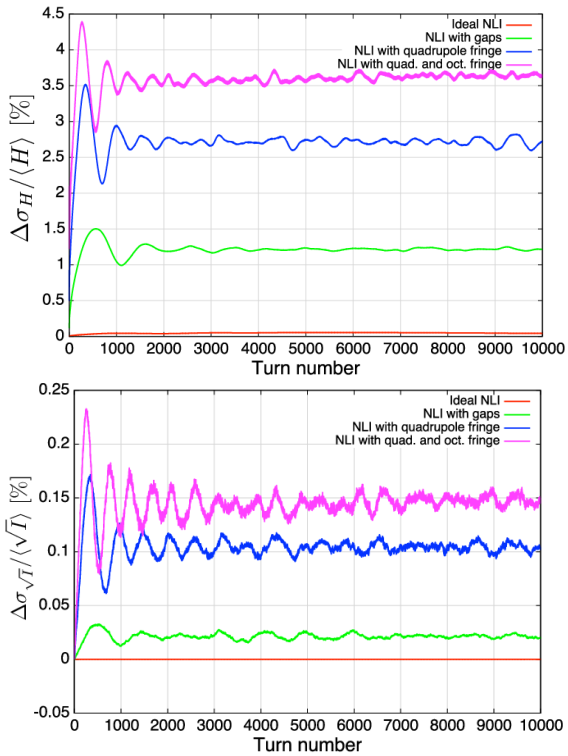

Figure 3: Evolution of the standard deviation within the beam of the two invariants of ideal single-particle motion [1].

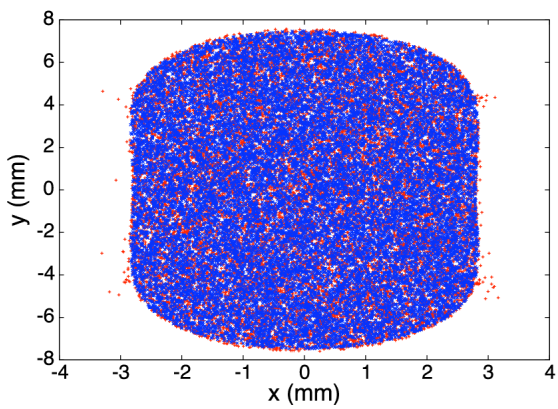

Figure 4: Final beam distribution after 10,000 turns. (Blue) Using the ideal nonlinear insert model (10). (Red) After including quadrupole and octupole fringe field corrections.

CONCLUSION

Symplectic tracking in the IOTA nonlinear magnetic insert for typical proton beam parameters, with quadrupole and octupole fringe field contributions added, indicates weak impact on beam quality with no evidence of instability. This study is made possible by the use of surface-fitting methods for smoothing numerical noise present in the original 3D finite-element magnetic field data. Future investigations will explore the use of more sophisticated symplectic integrators such as those described in [8] to correctly include contributions to $\vec{\mathcal{A}}_\perp$ due to terms containing $C_{2,s}^{[n]}$ and $C_{4,s}^{[n]}$ for $n \neq 0$.

ACKNOWLEDGMENT

This work was was supported by the Director, Office of Science, Office of High Energy Physics, of the U.S. Department of Energy under Contract No. DE-AC02-05CH11231, and made use of computer resources at the National Energy Research Scientific Computing Center.

REFERENCES

[1] V. Danilov and S. Nagaitsev, Phys. Rev. ST Accel. Beams **13**, 084002 (2010).

[2] S. Antipov *et al*, Journal of Instrumentation **12**, T03002 (2017).

[3] F. H. O'Shea *et al*, "Measurement of Nonlinear Insert Magnets," in Proc. PAC2013, Pasadena, CA, p. 922 (2013).

ISBN: 978-3-95450-184-7 doi:10.18429/JACoW-IPAC2018-THPAK036

[4] A. J. Dragt, *Lie Methods for Nonlinear Dynamics with Applications to Accelerator Physics*, University of Maryland (2011).

[5] C. Mitchell, "Complex Representation of Potentials and Fields for the Nonlinear Magnetic Insert of the Integrable Optics Test Accelerator," LBNL Paper LBNL-1007217 (2017).

[6] F. H. O'Shea, *private communication*

[7] C. Mitchell, "Numerical Tools for Modeling Nonlinear Integrable Optics in IOTA with Intense Space Charge Using the Code IMPACT-Z," in Proc. IPAC2018, Vancouver, Canada, THPAK035 (2018).

[8] Y. Wu, E. Forest, and D. Robin, Phys. Rev. E **68**, 046502 (2003).